J Mater Sci (2008) 43:952–959
DOI 10.1007/s10853-007-2197-2

Role of the rubber particle and polybutadiene cis content on the toughness of high impact polystyrene

Juliana Rovere · Carlos Alberto Correa · Vinícius Galhard Grassi · Marcus Fernando Dal Pizzol

Received: 20 July 2007 / Accepted: 28 September 2007 / Published online: 9 November 2007

Abstract High impact polystyrene (HIPS) is a classical reactor polymer blend produced by in situ polymerization of styrene in solution with polybutadiene rubber. The importance of the particle size and rubber crosslink density on the particle cavitation capability and the controlling of toughening mechanisms in the styrenic matrix is well established in current literature. In the present work, the role of the rubber particle on the HIPS toughness has been investigated for two commercial grades with low and high cis polybutadiene. Transmission electron microscopy (TEM) was employed for observation of particle size distribution and digital imaging applied for quantitative analysis of the micrographs. Measurements of apparent volume fraction and average particle size were determined in TEM images for both grades, while the gel content and swelling index were employed to evaluate the effect of the polybutadiene cis isomer on the rubber crosslink density. Grade morphology and crosslink effects on mechanical properties were assessed by slow three-point bending and uniaxial tensile testing. The results illustrate that polybutadiene cis content in HIPS grades has strong influence on the mechanical properties, particularly affecting yielding and energy to failure. Accordingly, it was observed that HIPS grades with equivalent average particle size and apparent volume fractions present a much higher energy to failure and a lower yield stress with high cis content polybutadiene when compared to their lower cis polybutadiene counterparts.

J. Rovere · C. A. Correa (✉)
Laboratório de Blendas e Compósitos Termoplásticos, Universidade São Francisco, Rua Alexandre Rodrigues Barbosa, 45, Itatiba, SP CEP 13251-900, Brazil
e-mail: carlos.correa@saofrancisco.edu.br

J. Rovere
e-mail: ju_rovere@yahoo.com.br

V. G. Grassi · M. F. D. Pizzol
Innova S.A, Rod. Tabaí/Canoas, BR 386, km 419, Polo Petroquímico de Triunfo, Triumph, RS CEP 95853-000, Brazil
e-mail: vinicius.galhard@petrobras.com

M. F. D. Pizzol
e-mail: marcus.dalpizzol@petrobras.com

Introduction

The tendency of many polymeric materials to undergo brittle fracture, especially in notched impact tests, has made the rubber toughening of plastics and its relationship with polymer composition and microstructure a major issue in polymer science. In general, the fracture resistance of a typical glassy polymer such as polystyrene (PS) can be substantially improved by incorporating a dispersed rubber phase, leading to a well-known class of materials named high impact polystyrene (HIPS) [1]. This class is known as a typical rubber toughened polymeric material basically prepared by the free-radical polymerization of styrene in the presence of dissolved polybutadiene (PB) to improve the impact strength and toughness of glassy polystyrene matrix. Major consumer applications of HIPS grades include packaging, containers, appliance parts, housewares, and interior parts in household electronics [2, 3].

HIPS materials are comprised of multicomponent and multiphase polymeric materials, with glassy and rubbery phases, and thus end-use properties are dependent on many parameters [4, 5], as shown in Table 1. A number of factors, related to the rubber component, have been identified as affecting the toughness of these systems, including the volume fraction of the rubber phase, its chemical composition,

Table 1 Molecular and morphological parameters that influence technical properties [6]

Matrix	Finished article	Soft component
Molecular weight	Stiffness	Type of rubber
Molecular weight distribution	Toughness	Phase-volume ratio
Additives	Flowability	Particle size
	Heat distortion	Particle size distribution
	Stress crack resistance	Particle morphology
	Gloss	Degree of grafting
	Transparency	Crosslinking density
	Weathering resistance	Cis content

degree of crosslinking, particle morphology, level of adhesion to the matrix, type of rubber, and most importantly the rubber particle size and its size distribution [6].

Advances in polymer chemistry allowed manufacturing of rubber toughened materials with different kinds of rubber morphology. In the particular case of HIPS, the rubber phase is a composite structure consisting of bulk rubber with PS subinclusions [7]. In most cases, the rubber used is polybutadiene, although styrene–butadiene copolymers and ethylene–propylene-copolymers (EPDM) are also recommended depending on the purpose. Particle size and morphology are determined during the phase inversion in the polymerization process and mass polymerization tends to lead to a quite broad distribution of *salami* or multiple inclusion particles [8]. The bulk process consists of polymerizing styrene in the presence of dissolved rubber with polystyrene chains being formed within the homogeneous rubber solution. The second phase can be produced during the polymerization of the matrix or formed during the final manufacturing steps in the case of polymer blends obtained by melt mixing [9]. The system then separates into two phases after a few percent of conversion, because the two polymer solutions are immiscible. The monomer is distributed between the two phases (polystyrene–styrene and rubber–styrene). Owing to the fact that the amount of polystyrene increases with conversion and the amount of rubber remains constant, the polystyrene phase increases in volume at the expense of the rubber phase [6]. When the phase-volume ratio approaches unity, phase inversion begins, and the rubber phase is distributed within the surrounding polystyrene phase [10, 11]. The viscosity of the system increases in the same way, and the rubber-phase droplets become fixed in size at roughly 30–35% conversion [12]. Conversion is then carried out to a high level, and the residual monomers and solvent are removed. Phase inversion can be observed with a phase-contrast microscope [13] and by viscosity measurements [14].

On the other hand, emulsion polymerization leads to the so-called *onion* or core-shell structures usually from triblock copolymers styrene–butadiene–styrene (SBS) or diblock styrene–butadiene (SB), which presents a smaller particle size and less dispersed distribution. Another physical method for controlling morphology and concomitantly improving interface properties is the addition of block copolymers to the system. Depending on their composition, chemical structure, and dispersion conditions, a myriad of particle morphologies can be attained [8]. Most of them are reported in a review by Echte [6].

Generally, it is difficult to isolate the effect of changes in rubber particle internal structure from particle size and distribution itself. Many studies supported by microscope techniques have provide enough evidences to support that the rubber particles are responsible for promoting multiple crazing mechanism in the polystyrene matrix by acting as stress concentrators during the craze initiation, thereby permitting substantial plastic deformation to occur prior to failure. This is particularly true when considering that no improvement in toughness is achieved in glassy thermoplastics modified with rigid particles [15, 16].

The characteristic HIPS morphology can be successfully elucidated by optical and electron microscopy. Chemical, dynamic and thermomechanical analysis (DMTA) and differential scanning calorimetry (DSC) are used for further information on the dual-phase polymer structure. The utilization of either of scanning or transmission electron microscopy (TEM) for characterization of such systems is quite interesting, given that it is a quite straightforward and accurate technique [17]. In TEM analysis, the specimen preparation is a critical step and sophisticated ultramicrotomy has to be used to prepare slices in the range 70–100 nm. Contrast between the phases is achieved by staining one of the components with a heavy compound to increase differences in electron density. Osmium tetroxide (OsO_4) has been reported as an efficient rubber staining agent for HIPS and ABS with excellent phase-contrast results. Moreover, the advance of modern digital image analysis allows quantitative measurements on morphological parameters with the aid of computer techniques [9]. The effects of these morphologies on the mechanical properties of modified polymers are as of yet not fully understood. However, it is known that the

size of the rubber particles influences the fracture behavior of the polymers [18, 19].

The drop in yield stress scales with particle size, volume fraction, and rubber crosslink density in rubber toughened plastics [20]. The apparent volume fraction can be estimated by electron microscopy when the effective area occupied by the particles divided by the whole micrograph area is known [8]. Several works have also shown a close relationship between rubber crosslink density and polybutadiene cis content [21–23].

The characterization of polybutadiene in HIPS can be realized through the determination of gel content that represents the insoluble fraction of HIPS in toluene/methylethylketone (MEK), according to the Ruffing technique of phase separation [24].

The high cis polybutadiene produces HIPS with lower crosslink density in the rubber phase, which improves impact strength [25]. The isomer content in high cis polybutadiene varies between 95 and 98% [26]. Techniques such as Fourier transform infrared spectroscopy (FTIR) and nuclear magnetic resonance spectroscopy (NMR) are used to quantify the cis isomer content in polybutadiene [26–30].

The main advantage of FTIR spectroscopy for polymer analysis is that it is a nondestructive technique and the samples are analyzed in bulk, either by transmission or by attenuated total reflectance (ATR) [31].

In the present work, the role of the rubber particle size and the rubber crosslink density on the toughness of HIPS are investigated for two commercial grades containing low and high cis polybutadiene content.

Experimental details

Materials

Two commercial HIPS grades were supplied by Innova S.A containing about 5.1–5.5 wt% of polybutadiene, which are specified as HIPS1 and HIPS2. They were chosen as the parental composition for this study. The choice considered differences in rubber average particle size distribution, while the particle internal morphology was the same—the well-known multiple inclusion or *salami* particles. A summary of the general properties measured by means of standard characterization methods (described in table footnotes) for the materials studied are reproduced in Table 2.

The most important industrial processes for manufacturing polybutadiene employ anionic (butyl-lithium) or coordination polymerization (mainly cobalt- or neodymium-based systems) [32]. In the present work, two commercial types of rubbers were used in HIPS grades, basically polybutadienes with varying viscosities and different proportions of the isomer configurations *trans*-1,4, *cis*-1,4, and vinyl-1,2. The neodymium process yields the so-called linear high cis polybutadienes, with the isomer *cis*-1,4 content within 96 and 98% [25].

Table 2 General properties of the HIPS samples studied

Properties	Unit	Material	
		HIPS1	HIPS2
Mw × 10^{-3}[a]	g/mol	172	185
Mz × 10^{-3}[b]	g/mol	239	270
Mw/Mn[c]	–	1.9	1.88
Gel content[d]	%	18.1	11.8
Swelling index[e]	–	11.8	24.5
Mineral oil[f]	%	0.6	1.0
PB (*[g] and #[h])	%	5.1#	5.5*
Cis-PB content[i]	–	Low	High

[a] Mw: weight-average molecular weight of PS (g/mol) as determined by gel permeation chromatography (G.P.C.)

[b] Mz: z molecular weight of PS (g/mol)

[c] Mw/Mn: distribution molecular weight

[d] Gel content: second-phase weight fraction (%) measured by phase separation methods in selective solution (the samples were dissolved and washed in methyl ethyl ketone (MEK) and toluene solution (proportion 43:57, vol.), the insoluble part was separated by centrifugation, precipitated by ethanol, centrifuged and then filtered, dried and weighed

[e] Swelling index: weight ratio between swollen and dry gel (%). The dry gel is measured by phase separation methods in a selective solvent (toluene); the sample swelling index in toluene is given by the ratio of the swollen and the dry gel weight

[f] Mineral oil: measured by FTIR method

[g] PB*: weight fraction of PB (%) measured by titration methods

[h] PB#: weight fraction of PB (%) measured by FTIR method

[i] Polybutadiene cis content: measured by FTIR or NMR

Methods

The materials were compression moulded at 195 °C into 4-mm thick sheets and compression loads of 150–1,000 kgf. After each moulding cycle the sheets were cooled down until 30 °C. The equipment used to make the compression moulded sheets was a Mecanoplast, model PLR 25. Specimens for mechanical testing were cut from these sheets.

Morphological and image analysis

Image analysis of TEM micrographs was used to characterize the selected grades in terms of their rubber particle *apparent* volume fractions, Φ_A, and particle average diameter, D_{eq}. The particle minimum count (N) that must

be utilized to calculate the average particle diameter is specific to each system, as quoted earlier in the literature [33]. Accordingly, suitable particle count should be above 200. In the present work, five micrographs were analyzed for each sample, independent of the number of particles in the micrographs. The polymer morphologies by TEM were studied using a Philips electron microscopy, model EM208S operating at 80 kV. Osmium tetroxide was used as the fixing and staining medium. Polymer samples with a thickness of about 100, 120, and 150 nm were prepared using a Leica ultramicrotome, model UCT Ultracut. The results are presented in terms of the average three film thicknesses utilized. The softwares used to image analysis were Jasc Paint Software, of Jasc Software, and JMicro Vision, of Nicolas Roduit.

Quantitative analysis of cis in polybutadiene using FTIR

The FTIR spectra were obtained using a Nicolet equipment, model Avatar 360. The films were prepared from a solution in chloroform, 2% vol., and laid upon a KBr cell. Each isomer content was obtained from the absorbancies in 965 cm^{-1} (*trans*-1,4), 911 cm^{-1} (vinyl-1,2), and 727 cm^{-1} (*cis*-1,4), according to the Kimmer [34] method, which considers the sum of each isomeric unity proportion related to the total amount of double bonds (C=C absorbencies in 1,637 cm^{-1} for low cis and 1,653 cm^{-1} for high cis).

Uniaxial tensile tests

The main parameters from uniaxial tensile tests were determined from stress–strain diagrams. The testing equipment was an Instron, model 5569. Specimens for mechanical testing were milled from the moulded sheets into dumbbell specimens with width $W = 10.12$ mm; thickness $B = 4.0$ mm, and length $L = 170$ mm. The tests were carried out using a crosshead speed of 50 mm/min in a controlled room temperature of 23 °C according to ISO-527. An average of five specimens were taken for each sample.

Slow three-point bending tests

Slow three-point bending tests were performed in an Instron testing machine, model 5569, to determine the Young's modulus (E). Specimens for mechanical testing were milled from the moulded sheets into single edge notched bars (SENB) with width $W = 4.0$ mm; thickness $B = 12.70$ mm, and length $L = 64.00$ mm according to ISO-178. The tests were carried out using a crosshead speed of 10 mm/min in a controlled room temperature of 23 °C. An average of five specimens were taken for each sample.

Results and discussion

TEM characterization and quantitative particle analysis

On image processing, the gray image is transformed into a digital binary image in such a way that the ratios between the dark and bright areas can be determined and processed by computing routines in the image analyser.

After the image processing, the reference parameters—rubber particle *apparent* volume fractions, Φ_A, and particle average diameter, D_{eq}—were measured. The Φ_A is obtained by dividing the area occupied by rubber particle (A_R) by the total area on the micrograph (A_T) (Eq. 1). The parameter D_{eq} is calculated according to Eq. 2, where A is the area occupied by the particle.

$$\Phi_A = \frac{\sum A_R}{\sum A_T} \tag{1}$$

$$D_{eq} = 2\sqrt{\frac{A}{\pi}} \tag{2}$$

The histogram that represents the particle size spectrum was obtained dividing the spectrum in 20 D_{eq} bins as a function of the frequency count observed. The main parameters used in the process are shown in Eqs. 3–5, showing how the parameters were calculated.

$$Dn = \frac{\sum NiDi}{\sum Ni} \tag{3}$$

$$Dw = \frac{\sum NiDi^2}{\sum DiNi} \tag{4}$$

$$DD_{eq} = \frac{Dw}{Dn} \tag{5}$$

where Di = particle mean diameter within the bin; Dn = numerical particle mean diameter; Dw = weight particle mean diameter; and DD_{eq} = particle diameter distribution.

The DD_{eq} parameter was calculated based upon the statistical concept of dispersivity of the particle size distribution. This parameter is a measure of the particle equivalent diameter distribution, i.e., the farther DD_{eq} is from the unity, the wider the particle size spectrum is, and hence the more heterogeneous the sample is.

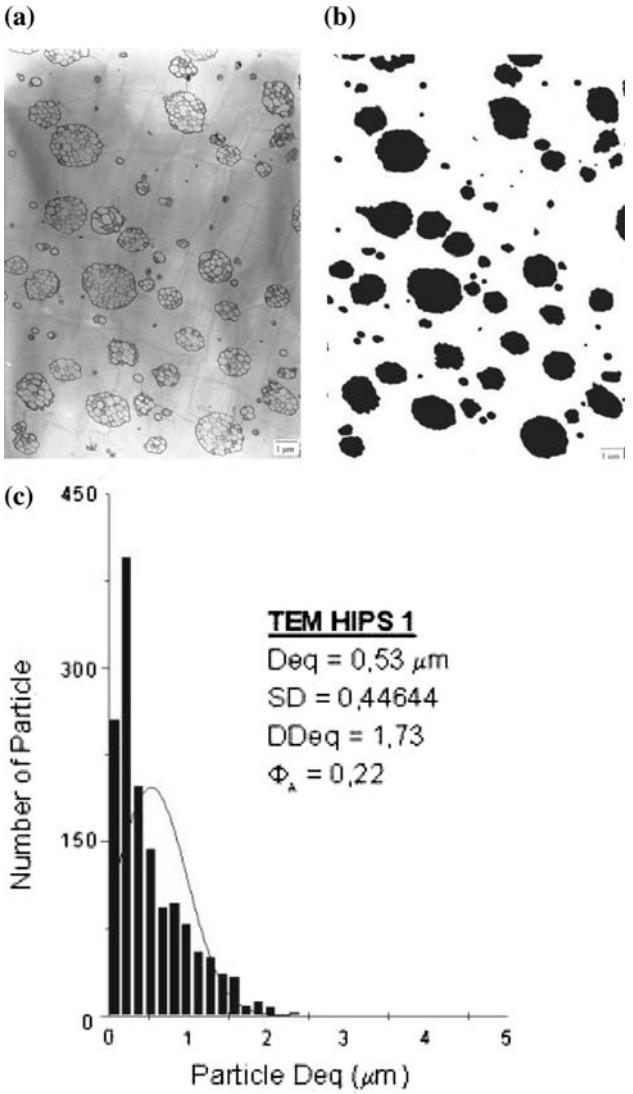

Fig. 1 (**a**) TEM micrograph of HIPS1 with (**b**) corresponding binary image obtained from digital image analysis and (**c**) corresponding particle size histogram

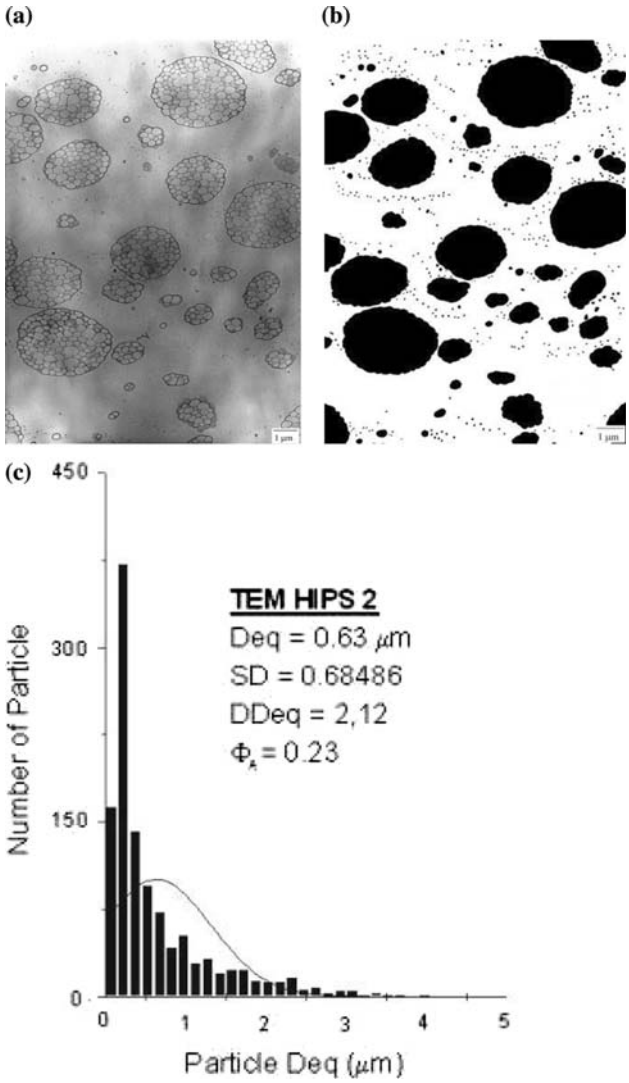

Fig. 2 (**a**) TEM micrograph of HIPS2 with (**b**) corresponding binary image obtained from digital image analysis and (**c**) corresponding particle size histogram

In Fig. 1a, the morphology observed by TEM is illustrated for HIPS1. The corresponding binary image obtained from digital image analysis is depicted in Fig. 1b, and the corresponding histogram of the particle diameter distribution is depicted in Fig. 1c.

In Fig. 2a, the morphology observed by TEM is illustrated for HIPS2. The corresponding binary image obtained from digital image analysis is depicted in Fig. 2b, and the corresponding histogram of the particle diameter distribution is depicted in Fig. 2c.

According to Figs. 1b and 2b, the results of the particle size analysis by TEM for HIPS1 and HIPS2 are shown in Table 3.

The apparent volume fraction Φ_A and equivalent particle diameter D_{eq} obtained for both HIPS1 and HIPS2 are basically equivalents. The only difference observed on the particle diameters histogram for both materials is the broadness of the spectra, as measured by DD_{eq}. Therefore, the changes in mechanical properties shall be evaluated in terms of the rubber crosslink density, i.e., the swelling index. It is relevant to point out that the gel content values presented in Table 2 do not correlate with Φ_A once it is influenced by the trapped occluded PS within the particle and consequently by the rubber crosslink density, as discussed in the current literature [9, 35].

Quantitative analysis of cis in polybutadiene using FTIR

Figure 3 illustrates the polybutadiene spectra obtained for (a) HIPS1 and (b) HIPS2. Their comparison shows that

Table 3 Results of the particle analysis by TEM

TEM							
D_{eq} (μm)		DD_{eq}		N		Φ_A	
HIPS1	HIPS2	HIPS1	HIPS2	HIPS1	HIPS2	HIPS1	HIPS2
0.53	0.63	1.73	2.12	1468	1152	0.22	0.23

D_{eq} = average of equivalent particles diameter in histogram;
N = particle count; DD_{eq} = particle size distribution;
Φ_A = rubber particle *apparent* volume fractions

the intensity of cis band peak in Fig. 3a is lower than the cis band peak in Fig. 3b. The height of the peak is related to the isomer content. Quantitative analysis of the FTIR spectra from the pure polybutadiene rubbers used to produce HIPS indicates that HIPS1 (low cis) has 35% cis content and HIPS2 (high cis) has 98% cis content.

The polybutadiene analysis is important because its chemical structure influences the final properties of HIPS. The so-called high cis polybutadyene (HIPS2) favors a lower rubber crosslink density as it contains a very low amount of the vinyl-1,2 isomer, which is the most active site for crosslink structures. As a result, HIPS containing this type of rubber usually presents high impact strength even at low temperatures. The high cis configuration presents a much lower sub-ambient glass transition around –100 °C, while for a low cis configuration the glass transition is –78 °C [21]. On the other hand, the high cis configuration may reduce the grafting level and impair the mechanical properties [36].

Mechanical properties

The results of the mechanical testing for HIPS1 and HIPS2 are summarized in Table 4 for tensile properties, and in Table 5 for flexural properties.

In Fig. 4, the stress–strain diagram is depicted for uniaxial tensile tests and in Fig. 5 for slow three-points bending tests. The plots represent an average curve of all specimens tested.

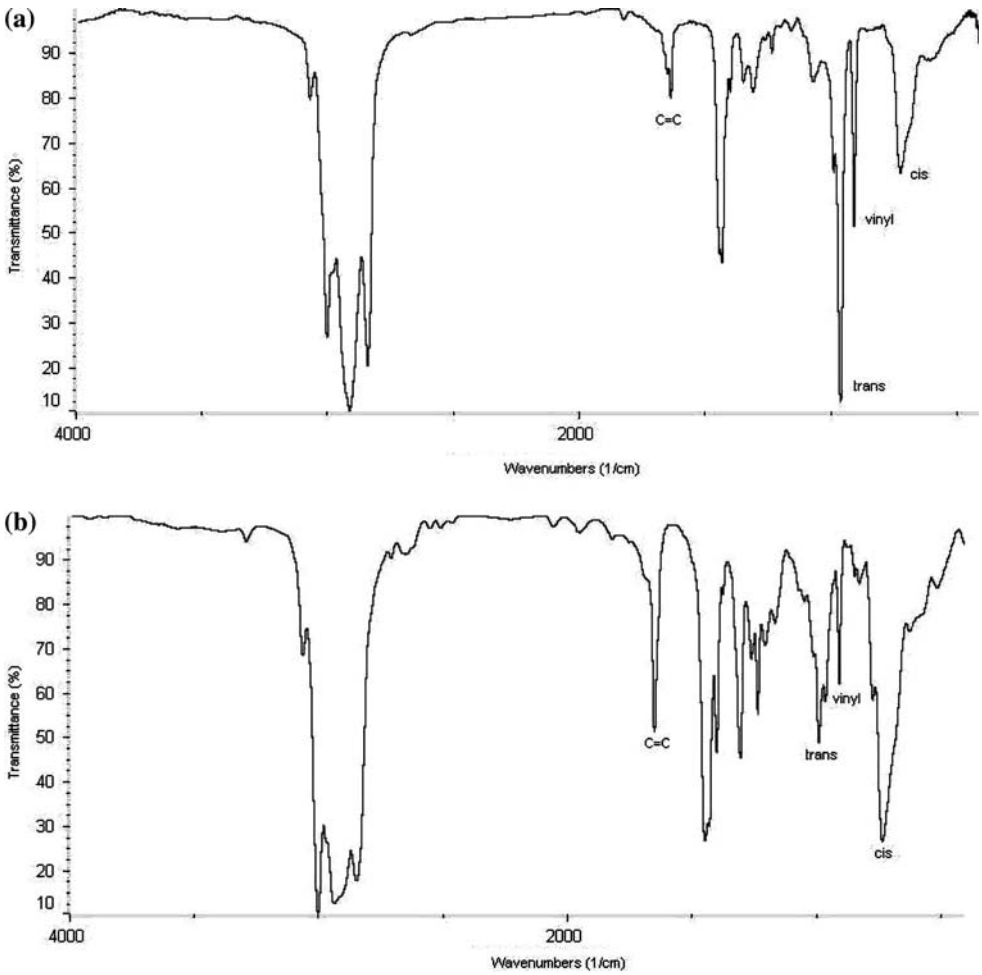

Fig. 3 Polybutadiene spectra for (**a**) HIPS1, low cis content, and (**b**) HIPS2, high cis content

Table 4 HIPS tensile properties

Propriety		ISO		Typical values	
		Standard	Unit	HIPS1	HIPS2
1	Modulus (E)	ISO-527	GPa	2.07 ± 0.08	1.76 ± 0.06
2	Tensile strength (at failure), σ_f	ISO-527	MPa	20.25 ± 0.47	16.56 ± 0.40
3	Tensile strength (at yield), σ_y	ISO-527	MPa	24.02 ± 0.53	20.02 ± 1.21
4	Strain (at failure), ε_f	ISO-527	%	17.10 ± 4.61	34.55 ± 4.17
5	Strain (at yield), ε_y	ISO-527	%	1.32 ± 0.08	1.17 ± 0.08

Table 5 HIPS flexural properties

Propriety		ISO		Typical values	
		Standard	Unit	HIPS1	HIPS2
1	Flexural strength (at maximum load)	ISO-178[a]	MPa	46.18 ± 1.11	43.68 ± 0.69
2	Strain (at maximum load), ε_{max}	ISO-178[a]	%	1.91 ± 0.16	1.97 ± 0.01
3	Strain (failure), ε_f	ISO-178[a]	%	7.14 ± 2.01	10.02 ± 0.01
4	Energy (break)	ISO-178[a]	J	0.23 ± 0.03	0.33 ± 0.01

[a] Slow three-point bending tests were carried out based upon ISO-178 standard, on regard to sample dimensions

HIPS1 achieves a higher tensile yield stress than HIPS2, and it presents a much lower average strain to failure than HIPS2, as depicted in Fig. 4. In slow three-points bending tests, the same trend was observed with a reduction in total energy to failure for HIPS1 compared to HIPS2. However, the maximum load that corresponds to the energy required to initiating the crack is basically the same for both materials. This correlates with the tensile yield stress data. So the difference remains on the energy required to propagate the crack, as materials demonstrate an equivalent particle diameter and apparent volume fraction.

Basically, the cis content in polybutadiene is related to the crosslink density, and according to the swelling index presented earlier in Table 2 for both materials (HIPS1 = 11.8 and HIPS2 = 24.5), a high cis content implies in a low crosslink under controlled devolatilization conditions. On the other hand, previous work has shown a close relationship between toughness and rubber crosslink density in rubber toughened polystyrenes as cavitation processes within the rubber are responsible for delayed yielding. In the present work, HIPS with high cis content, and consequently, a low crosslink density presents a higher energy to fracture in both mechanical tests, which correlates with results presented in the current literature [20, 37].

Conclusions

The present study has expounded that digital image analysis can be powerfully used for quantitative measurements

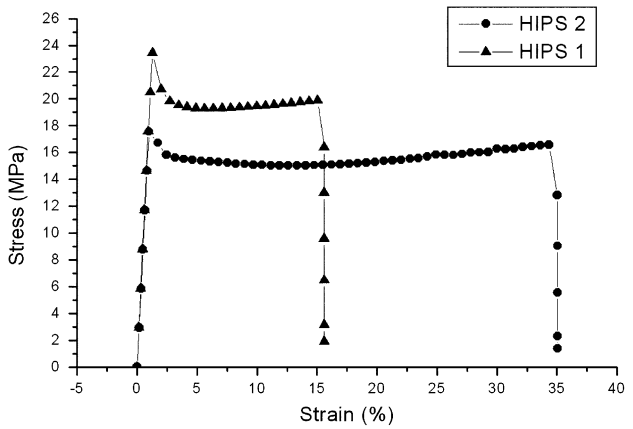

Fig. 4 Stress–strain plot for HIPS1 (▲) and HIPS2 (●) in uniaxial tensile tests

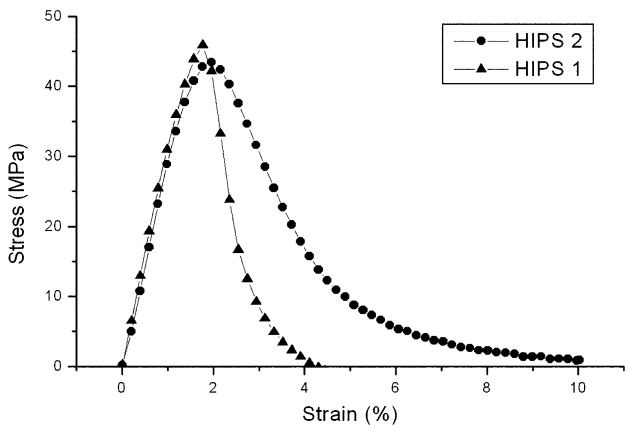

Fig. 5 Stress–strain plot for HIPS1 (▲) and HIPS2 (●) in slow three–points bending

on TEM micrographs of dual-phase polymers systems such as high-impact polystyrene. Therefore, HIPS properties can be statistically expressed in terms of particle size, size distribution, and apparent volume fraction. The present work also yields further evidences for understanding the role of rubber particles in HIPS toughening mechanism, particularly on the effects of the polybutadiene cis content on controlling the crosslink density within the rubber phase.

The polybutadiene cis content has strong influence on the mechanical properties of HIPS grades, particularly affecting yielding and energy to failure in tensile and slow three-point bending tests. Accordingly, HIPS grades with equivalent average particle size and apparent volume fractions presented a much higher energy to failure and a lower yield with high cis content polybutadiene, when compared to the HIPS with low cis content polybutadiene. The results are consistent with current literature on rubber toughening of HIPS considering that yield stress and energy to fracture are dependent on particle size and rubber crosslink density will be controlled by the polybutadiene cis content.

Acknowledgements The authors would like to thank the Materials Engineering Department at UFSCar for their kind support with mechanical testing and Innova Petrochemicals S.A. from Brazil for supplying the materials, facilities, and for the MSc degree research grants for Mrs. Juliana Rovere.

References

1. Bucknall CB (1977) Toughened plastics. Applied Science Publishers, London, p 1
2. Lee SJ, Jeoung HG, Ahn KH (2003) J Appl Polym Sci 89:3672
3. Zhang J, Wang X, Lu L, Li D, Yang X (2003) J Appl Polym Sci 87:381
4. Morales G, Leon RD, Acuña P, Flores RF, Robles AM (2006) Polym Eng Sci 46:1333
5. Aiamsen P, Paiphansiri U, Sangribsub S, Polpanich D, Tangboriboonrat P (2003) Polym Int 52:1198
6. Echte A (1989) In: Riew CK (ed) Rubber-toughened plastics. American Chemical Society, Washington, p 15
7. Grassi VG (2002) Dissertação de Mestrado. Universidade Federal do Rio Grande do Sul, Brazil
8. Correa CA, de Sousa JA (1997) J Mater Sci 32:6539
9. Maestrini C, Merlotti M, Vighi M, Malaguti E (1992) J Mater Sci 27:5994
10. Molau GE (1965) J Polym Sci Part A-1 4235:12, 67
11. Molau GE, Kesskula H (1966) J Polym Sci Part A-1 4:1595
12. Bender BW (1965) J Appl Polym Sci 9:2887
13. Echte A (1977) Angew Makromol Chem 58/59:175
14. Riess G, Gaillard P (1983) In: Reichert KH, Geiseler W (eds) Polymer reaction engineering. Hanser, Munich, p 221
15. Kinloch AJ, Young RJ (1983) Fracture behavior of polymers. Applied Science Publishers, London, p 496
16. Serpooshan V, Zokaei S, Bagheri R (2007) J Appl Polym Sci 104:1110
17. Correa CA (1995) Polímeros: Ciência e Tecnologia Jan/Mar:24
18. Hobbs SY (1986) Polym Eng Sci 26:74
19. Katime I, Quintana JR, Price C (1995) Mater Lett 22:297
20. Bucknall CB, Soares VLP (2004) J Polym Sci Part B: Polym Phys 42:2168
21. Sardelis K, Michels HJ, Allen G (1983) J Appl Polym Sci 28:3255
22. Rivera MR, Herrera R, Benvenuta JJ, Ríos L (2005) J Elast Plast 37:267
23. Rivera MR, Herrera R, Benvenuta JJ, Ríos L (2006) J Elast Plast 38:133
24. Ruffing NR (1966) Process for making graft copolymers of vinyl aromatics compounds and stereospecific rubbers. US Patent 3,243,481
25. Dal Pizzol MF (2005) PhD thesis, Universidade Federal do Rio Grande do Sul, Brazil
26. Pires NMT, Lira CH, Ferreira AA, Coutinho PL, Nicolini PL (2001) In: ABTB (ed) Anais do 9° Congresso Brasileiro de Tecnologia da Borracha, São Paulo, Brasil, November 2001, p 1
27. Lacoste J, Delor F, Pilichowski JF, Singh RP, Prasad AV, Sivaram S (1996) J Appl Polym Sci 59:953
28. Silas RS, Yates J, Thornton V (1959) Anal Chem 31:529
29. Mello IL, Soares BG, Coutinho FMB, Nunes DSS (2007) Polímeros: Ciência e Tecnologia 17(1):62
30. Canto LB, Mantovani GL, Azevedo ER, Bonagamba TJ, Hage E, Pessan LA (2006) Polym Bulletin 57:513
31. Grassi VG, Forte MC, Dal Pizzol MF (2001) In: Proceedings of IUPAC World Polymer Congress, Beijing, China, July 2001, v. 1, p 398
32. Mello I, Coutinho F, Soares B (2004) Química Nova 27(2):277
33. Correa CA, Yamakawa RS, Horiuchi LN, Canevarolo SV (1998) In: Anais do 13° Congresso Brasileiro de Engenharia e Ciência dos Materiais (CEBCIMAT),Curitiba, PR, Brasil, December 1998, p 4068
34. Schroder GM, Arndt KF (1988) Polymer characterization. Hanser Publishers, Munich, p 215
35. Anzaldi S, Bonifaci L, Malaguti E, Vighi M, Revanetti GP (1994) J Mater Sci Lett 13:1555
36. Bayer (2003) Polybutadiene: structure and properties. Brochura técnica 1
37. Soares VLP (1994) PhD thesis, University of Cranfield, England